Synthesis of Platinum Nanowires in Organic−Inorganic Mesoporous Silica Templates by Photoreduction: Formation Mechanism and Isolation

Yuzuru Sakamoto,[‡] Atsushi Fukuoka,*[,†,‡] Takanori Higuchi,[‡] Noriyuki Shimomura,[†] Shinji Inagaki,[§] and Masaru Ichikawa*[,†,‡]

Catalysis Research Center, Hokkaido University, Sapporo 001-0021, Japan, Division of Chemistry, Graduate School of Science, Hokkaido University, Sapporo 060-0810, Japan, and Toyota Central R&D Labs., Inc., Nagakute, Aichi 480-1192, Japan

Received: September 2, 2003

Pt nanowires are synthesized in organic−inorganic mesoporous silica HMM-1 (channel diameter 3 nm) by photoreduction, and the formation mechanism and isolation of the wires have been studied. UV-irradiation of HMM-1 impregnated with H_2PtCl_6 for 48 h in the presence of adsorbed water and methanol leads to the formation of Pt nanowires (diameter 3 nm, length up to 5 μm) in the one-dimensional channels. On the other hand, H_2-reduction of H_2PtCl_6/HMM-1 at 443 K for 2 h results in the formation of Pt nanoparticles (diameter 3 nm) and short wires in the channels. The formation mechanism of the wires has been studied by transmission electron microscopy (TEM), X-ray absorption fine structure (XAFS), and powder X-ray diffraction (XRD), and it is suggested that Pt ions migrate in the water/methanol phase and are catalytically reduced on Pt particles to grow to wires. In the H_2-reduction, however, the reduction of Pt ions is faster than the migration, thus resulting in the formation of nanoparticles. The Pt wires are isolated by removing HMM-1 with HF treatment (yield 66%). The unsupported Pt wires are stabilized by ligands such as $[N(C_{18}H_{37})(CH_3)_3]Cl$ and $P(C_6H_5)_3$. Scanning tunneling microscope (STM) observation of the isolated Pt wires on highly oriented pyrolytic graphite (HOPG) confirms that the wires separated from HMM-1 have a necklace-like structure, while the wires from pure siliceous FSM-16 have a rodlike structure.

Introduction

In the emerging field of nanoscience and nanotechnology, metal nanowires are one of the key precursors to highly ordered nanostructures in the bottom-up approach.[1,2] The nanowires have great potential to show unique optical, magnetic, electrical, and chemical properties based on the anisotropic properties.[3] One of the most promising methods of preparing nanowires is the template synthesis, in which porous materials with uniform void spaces are used as a host to occlude the nanowires as a guest.[4]

Mesoporous silicas such as FSM-16,[5,6] MCM-41,[7] and SBA-15[8] have a great opportunity as a support of nanostructured metal due to large pores (2−50 nm) with a narrow distribution and a high surface area (up to 1000 $m^2\ g^{-1}$). Since the discovery of the mesoporous silicas, they have been used as supports to synthesize metal nanowires in the 1D channel structures.[9−15]

In our study of the ship-in-bottle synthesis of metal clusters in microporous zeolites,[16,17] we found that Pt nanowires were formed inside FSM-16 by the photoreduction of H_2PtCl_6 after adsorption of water and alcohol vapors on FSM-16.[18−24] Recently developed organic−inorganic hybrid mesoporous silicas are a new class of mesoporous materials containing organic groups in the framework,[25−31] and we studied the synthesis of nanowires by using the hybrid materials as supports. It was found that HMM-1 containing ethane fragments was a better support than FSM-16 for the preparation of long nanowires due to the well-ordered channel structure, and several mono- and bimetallic wires of Pt, Rh, Au, Pd, Pt−Rh, and Pt−Pd were synthesized in HMM-1 by the photoreduction method with good reproducibility.[32,33] The metal wires in HMM-1 have high crystallinity with uneven surfaces (nanonecklace structure), and Pt−Rh and Pt−Pd wires are alloy crystals.

Although much work has been devoted to the synthesis of metal nanowires in mesoporous templates such as silica,[9−15,18−24,32,33] alumina,[4,34,35] and carbon nanotube,[36−40] the formation mechanism of the metal nanowires has been less explored. Moreover, isolation of the nanowires from the templates is another important topic in the fabrication of well-ordered nanostructures from the wires as building blocks. It is known that the nanowires can be separated by dissolving the template materials with HF or NaOH,[10,11,14,15] but stabilization of the unsupported nanowires using ligands has been an important subject.

In this work, we have studied the formation mechanism of Pt nanowires in HMM-1 by means of transmission electron microscopy (TEM), X-ray absorption fine structure (XAFS), and powder X-ray diffraction (XRD). We propose the mechanism involving migration and reduction of Pt ions. The Pt wires are isolated by removal of silica matrix, and the unsupported wires have been characterized by high-resolution TEM (HR-TEM) and scanning tunneling microscopy (STM). We report the modification and stabilization of the Pt wires with ligands and the formation of Pt nanowire arrays.

* To whom correspondence should be addressed. E-mail address for A.F.: fukuoka@cat.hokudai.ac.jp. E-mail address for M.I.: michi@cat.hokudai.ac.jp.

† Catalysis Research Center, Hokkaido University.

‡ Division of Chemistry, Graduate School of Science, Hokkaido University.

§ Toyota Central R&D Labs., Inc.

10.1021/jp036617v CCC: $27.50
Published on Web 12/23/2003

Experimental Section

Chemicals. HMM-1 with $-CH_2CH_2-$ groups was prepared according to the literature method.[25] The BET surface area was 812 $m^2\ g^{-1}$, and the pore diameter was 3.1 nm. HMM-1 showed XRD peaks at $2\theta = 1.8°$, 3.1°, and 3.6° due to (100), (110), and (200) indices, characteristic of the 2D-hexagonal *p6mm* symmetry. $H_2PtCl_6 \cdot 6H_2O$, aqueous HF (ca. 46 wt %), and triphenylphosphine ($P(C_6H_5)_3$) were purchased from Wako Pure Chemicals. Octadecyltrimethylammonium chloride ($[N(C_{18}H_{37})(CH_3)_3]Cl$) was obtained from Tokyo Chemical Industry, and methanol and ethanol were obtained from Kanto Kagaku. All of the reagents were used as received.

Synthesis of Pt Nanowires in HMM-1. White powder of HMM-1 (200 mg) was dried under vacuum (ca. 10^{-3} Torr, 1 Torr = 133 Pa) at 373 K for 2 h. $H_2PtCl_6 \cdot 6H_2O$ (30 mg) was dispersed in deionized water (5 mL), and the solution was added to a slurry of HMM-1 in water (20 mL). After being stirred for 24 h, the mixture was evaporated to dryness and further dried under vacuum for 24 h. The resulting pale yellow powder, H_2PtCl_6/HMM-1 (Pt 5 wt %), was charged in a quartz cell and evacuated at 10^{-3} Torr for 24 h. H_2PtCl_6/HMM-1 was exposed to water vapor (ca. 20 Torr) for 2 h using the vacuum line technique and then to methanol vapor (ca. 100 Torr) for 2 h, and the sample was irradiated with a high-pressure mercury lamp (Ushio UM-102, 100 W, $\lambda = 250-600$ nm) at room temperature for 48 h. The cell temperature was kept at ca. 300 K by blowing air with a fan. A schematic diagram of the reaction setup for photoreaction is shown in Figure S1 in the Supporting Information. The powder sample in the quartz cell was stirred with a vibrator at 2−3 h intervals. After the irradiation, the resulting gray powder was dried under vacuum. On the other hand, H_2-reduction of H_2PtCl_6/HMM-1 was performed in flowing H_2 (20 mL min^{-1}) at 443 K for 2 h using a typical U-type glass reactor. Pt nanowires in FSM-16 were prepared according to our previous report.[21]

Isolation of Pt Nanowires from HMM-1. Aqueous HF (ca. 46 wt %) was diluted with ethanol to 2.5 wt %, and to this solution was added Pt/HMM-1 powder. After a few minutes, the solid powder was completely dissolved, and the solution turned pale gray. Unsupported Pt nanowires were separated with a filter paper and washed with ethanol (yield 66% based on the starting H_2PtCl_6). In some experiments, $[N(C_{18}H_{37})(CH_3)_3]Cl$ or $P(C_6H_5)_3$ was added to the HF solutions as a stabilizing ligand. For example, $P(C_6H_5)_3$ was dissolved in ethanol at 333 K, and after cooling to room temperature the aqueous HF solution was added ($P(C_6H_5)_3$ 1.5 wt %, ca. 10 times excess over bulk Pt atoms).

Characterization. XRD patterns were recorded on a Rigaku Miniflex using Cu Kα radiation ($\lambda = 0.154\,18$ nm) at 30 kV and 15 mA. TEM and HRTEM observations were performed with a Hitachi H-800 and a JEOL JEM-2000EXII, respectively, with an acceleration voltage of 200 kV. Energy-dispersive X-ray spectroscopy (EDS) analysis was carried out with a JEOL 2000ES, and the analysis spot was ca. 5 nm in diameter. For the TEM observation of unsupported nanowires, a copper microgrid was put in the HF solutions to deposit the wires, and the microgrid was washed with ethanol and dried in air.

XAFS spectra at the Pt L_{III} edge (11 562 eV) were measured at the BL-10B station in the Photon Factory of High Energy Accelerator Research Organization (KEK-PF, Tsukuba). The ring energy and current were 2.5 GeV and 200−300 mA, and the Si (311) channel cut monochromator was used. The Pt/HMM-1 sample was charged in an XAFS cell with KAPTON film windows, and spectra were measured at 296 K. XAFS data were analyzed by a REX2000 program (Rigaku). The k^3-weighted extended X-ray absorption fine structure (EXAFS) function χ was Fourier transformed into *R*-space using the *k*-range from 32.5 to 168.5 nm^{-1}. The inverse Fourier transform was calculated to obtain a filtered EXAFS function. The *R* range of the inverse Fourier transformation was taken from 0.12 to 0.33 nm. Phase shift functions and backscattering amplitudes for Pt−Pt, Pt−Cl, and Pt−O were extracted from the spectra of reference materials: Pt foil for Pt−Pt, Na_2PtCl_6 for Pt−Cl, and $Na_2Pt(OH)_6$ for Pt−O.

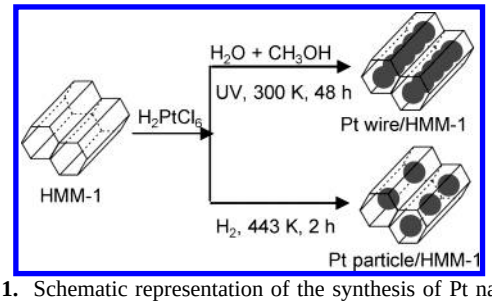

Figure 1. Schematic representation of the synthesis of Pt nanowires and nanoparticles in HMM-1.

STM observation was performed using a JEOL JSPM-5200. The ethanol solution of isolated Pt nanowires was deposited on a freshly cleaved highly oriented pyrolytic graphite (HOPG, ca. 8 mm × 8 mm), and the sample was dried in air. STM images were obtained in the constant-current mode with a Pt−Ir alloy tip, and the bias voltage and tunneling current were 1.2 V and 0.8 nA, respectively.

Results and Discussion

Synthesis and Formation Mechanism of Pt Nanowires in HMM-1. The main scheme of the synthesis of Pt nanowires and nanoparticles is illustrated in Figure 1. HMM-1 was impregnated with H_2PtCl_6 (Pt 5 wt %), and water and methanol vapors were added to the impregnated sample, H_2PtCl_6/HMM-1. UV irradiation of the sample for 48 h led to the formation of Pt nanowires. It is well-known that transition metal colloids are formed by radiochemical reactions in water/alcohol solutions, in which the reduction of metal salts takes place by solvated electrons and free radicals produced under irradiation.[41,42] We have applied this synthetic method in the solution phase to the reaction in solid mesoporous silica supports. In our method, adsorbed water and methanol work as solvents in the nanoscale void space, and methanol is a source of reducing agents under UV-irradiation (vide infra).

Figure 2 shows typical TEM images of the Pt wires and particles, and they are clearly seen as dark stripes and dots. The Pt wires are 3 nm in diameter in accord with the pore diameter of HMM-1 (3.1 nm), and the length ranges from 10 to several hundred nanometers reflecting the 1D channel structure (Figure 2b). This result indicates the formation of Pt wires inside the channels. In fact, almost no wire or particle is observed on the external surface of HMM-1. On the other hand, H_2-reduction of H_2PtCl_6/HMM-1 at 443 K for 2 h resulted in the formation of Pt particles with a diameter of 3 nm (Figure 2c). Short wires are also observed as a minor species in this sample. Other groups reported the formation of Pt wires by H_2-reduction of Pt ions.[10−13] In some cases, we also observed wires in the pore, but the formation of wire greatly depends on the reaction conditions such as a temperature program and a concentration of residual water. By comparison, the photoreduction is more reproducible to synthesize long Pt wires.

In the XRD patterns of Pt/HMM-1 (Figure 3), no significant change was observed at $2\theta = 1°-10°$ before and after the

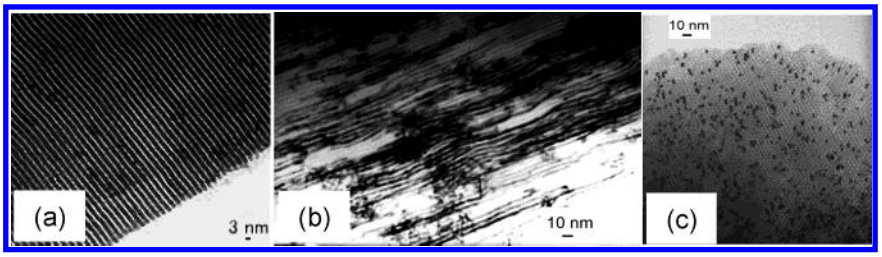

Figure 2. TEM images of (a) HMM-1, (b) Pt wire/HMM-1 synthesized by photoreduction, and (c) Pt particle/HMM-1 synthesized by H_2-reduction.

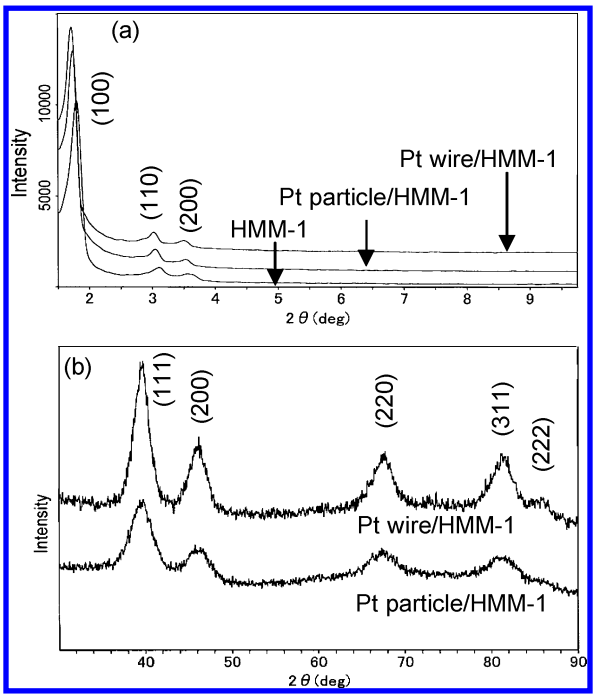

Figure 3. XRD patterns of HMM-1, Pt particle/HMM-1, and Pt wire/HMM-1 in (a) low 2θ angle and (b) high 2θ angle regions.

incorporation of metal, indicating that the pore structure of HMM-1 remained unchanged in the synthesis of the Pt wires. In the high 2θ region, typical peaks of fcc crystalline Pt are observed.

Mechanism for the formation of Pt nanowires in HMM-1 has been studied by changing the irradiation time. TEM images of the samples after irradiation for 0−48 h are shown in Figure 4. After 4 h, small Pt particles (up to 3 nm in size) are seen in the TEM image. Pt particles and short wires (mean length 10 nm) are observed after 8 h. Pt wires are clearly observed after irradiation of 12 h, and the mean length is 90 nm. The Pt wires grow longer by further irradiation for 24 and 48 h; the mean lengths are 120 and 220 nm, respectively. The XRD profiles of these Pt/HMM-1 samples also show the gradual formation of crystalline Pt with increased irradiation time (Figure S2 in Supporting Information).

The Pt/HMM-1 samples with various irradiation time were also characterized by XAFS. Figure 5 exhibits the Fourier transforms of k^3-weighted EXAFS functions $\chi(k)$ of Pt/HMM-1 and Pt foil. In the curve-fitting analysis of the peaks at 0.12−0.33 nm, the peaks were ascribed to Pt−Cl and Pt−Pt without the contribution of Pt−O (Table 1). Figure 6 exhibits the time evolution of coordination number (CN) of Pt−Cl and Pt−Pt in EXAFS analysis. It is found that the CN of Pt−Cl decreases linearly from 5.9 to 0.4 in 12 h, indicating that the reduction of H_2PtCl_6 is almost completed in 12 h. The CN of Pt−Cl is further decreased to ca. 0 in 48 h. On the other hand, the CN of Pt−Pt is increased from 0 to 8.2 in 12 h and then slightly increased to 9.1 in 48 h. Figure 6 also shows the mean length of wires in the TEM images. After the reduction is over at 12 h, the mean length of Pt wires is increased from 90 to 220 nm. This suggests that further growth of Pt wires takes place under UV-irradiation.

From the TEM and XAFS results, we propose the mechanism for formation of the Pt wires as shown in Figure 7. First, tiny Pt nanoparticles are formed in the mesoporous channels by the photoreduction of H_2PtCl_6. It is suggested that organic radicals such as $^{\bullet}CH_2OH$ are produced from adsorbed methanol under UV-irradiation[41,42] and the radicals reduce Pt salts. In fact, no reaction happened in the absence of methanol. When only methanol was adsorbed on H_2PtCl_6/HMM-1, reduction took place under irradiation but big Pt particles were formed as a major product on the external surface of HMM-1. Therefore, water is necessary as a cosolvent for the formation of wires inside the channels. The Pt ions are soluble in the water/methanol phase and can migrate in the channels to the surface of Pt particles. Then the Pt ions are catalytically reduced to grow nanowires. The TEM results of the samples after 12−48 h irradiation suggest that the Pt wires grow after the reduction of Pt−Cl is over. This may indicate that reduced Pt species such as radicals and tiny particles migrate and aggregate to form long nanowires. Hence the key to synthesizing the Pt wires is to promote the migration of Pt ion and small Pt species in the 1D channel. Under our H_2-reduction conditions, migration of Pt ion is difficult and growth of Pt nanoparticle to nanowire does not occur. If small amount of water remains after impregnation of Pt ions, Pt wires may be formed by facilitating the migration of Pt ions.[43] However, the formation of wires by

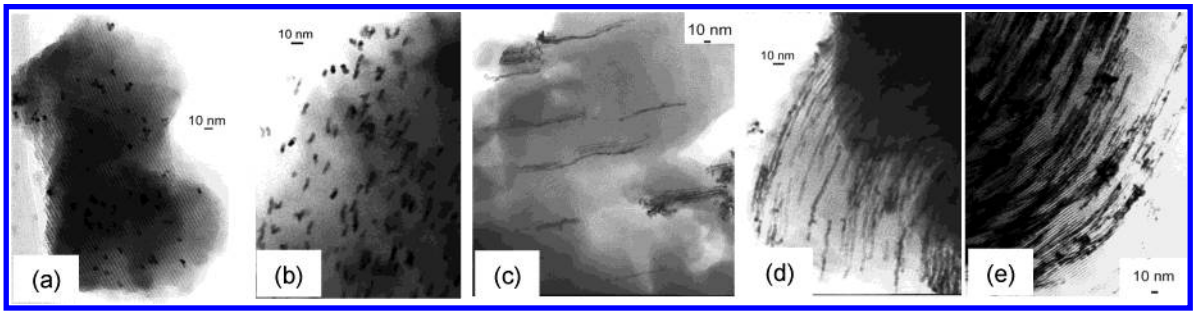

Figure 4. TEM images of Pt/HMM-1 after UV-irradiation for (a) 4, (b) 8, (c) 12, (d) 24, and (e) 48 h.

TABLE 1: Curve-Fitting Analyses of First Coordination Shells of Pt−Cl and Pt−Pt for Pt/HMM-1 after Various UV-Irradiation Times

sample	bond	CN[a]	R[b] (nm)	σ[c] (nm)	ΔE_0[d] (eV)	R[e] (%)
H_2PtCl_6/HMM-1	Pt−Cl	5.9 ± 2.0	0.232 ± 0.002	0.006	3.0	4.6
Pt/HMM-1 (4 h)	Pt−Cl	4.6 ± 2.0	0.231 ± 0.003	0.006	3.0	3.7
	Pt−Pt	0.5 ± 0.4	0.277 ± 0.004	0.007	6.6	
Pt/HMM-1 (8 h)	Pt−Cl	3.0 ± 0.6	0.230 ± 0.002	0.008	−0.2	7.2
	Pt−Pt	2.0 ± 0.6	0.275 ± 0.006	0.008	−1.3	
Pt/HMM-1 (12 h)	Pt−Cl	0.4 ± 0.4	0.233 ± 0.006	0.007	−1.5	4.2
	Pt−Pt	8.2 ± 0.8	0.276 ± 0.001	0.007	−1.5	
Pt/HMM-1 (24 h)	Pt−Cl	0.5 ± 0.5	0.233 ± 0.001	0.007	5.3	4.2
	Pt−Pt	8.2 ± 1.0	0.276 ± 0.001	0.007	1.0	
Pt/HMM-1 (48 h)	Pt−Pt	9.0 ± 2.0	0.276 ± 0.002	0.007	0.6	4.9
Pt foil	Pt−Pt	12.0 ± 2.0	0.277 ± 0.002	0.006	−0.2	0.5

[a] Coordination number. [b] Interatomic distance. [c] Debye−Waller factor. [d] Correction of threshold energy. [e] Residual factor.

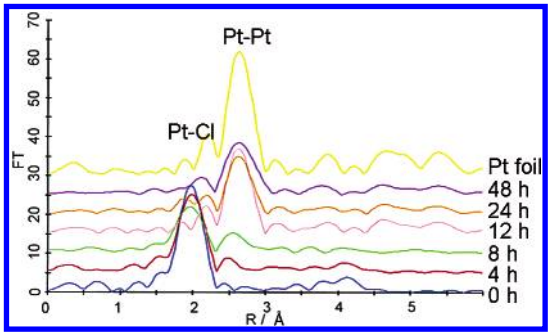

Figure 5. Fourier transforms of $k^3\chi(k)$ for Pt/HMM-1 after various UV-irradiation times.

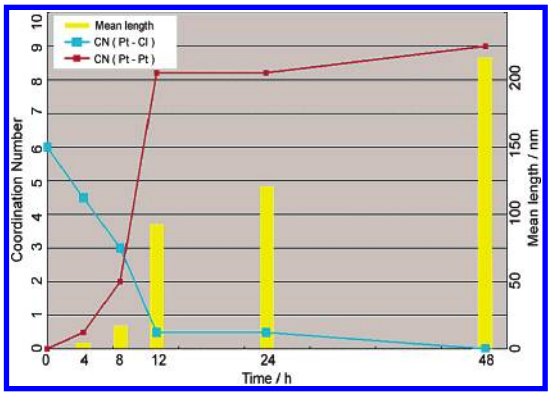

Figure 6. Time evolution of coordination numbers of Pt−Cl and Pt−Pt in EXAFS and mean length of Pt wires in TEM.

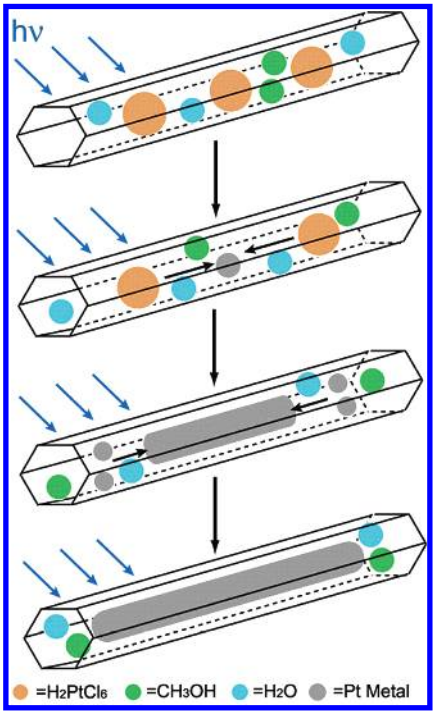

Figure 7. Proposed mechanism for the formation of Pt wires in HMM-1.

H_2-reduction needs careful control of reaction conditions as described in the synthesis section.

Isolation of Pt Nanowires. Pt nanowires were separated by dissolving siliceous HMM-1 with diluted aqueous HF solution. The Pt wires were isolated as a solid in a Pt yield of 66%. Figure 8a is a typical TEM image of the unsupported Pt wires, and the EDS analysis confirmed the removal of Si. Figure 8b is a low-magnification TEM image, and the wires aggregate to form a bundle. However, each nanowire keeps its original structure without fusion, and the length is ca. 5 μm, and the aspect ratio is 1600. The length of the wires can be accurately measured by removing the support. The Pt wires were stable as a solid at 278 K, but in ethanol suspension, the wires aggregated to form big Pt particles (ca. 20 nm) in 2 days at 278 K.

To modify the unsupported Pt wires, surfactants and tertiary phosphines such as $[N(C_{18}H_{37})(CH_3)_3]Cl$ and $P(C_6H_5)_3$ were added to the HF solution. Figure 8c is a TEM image of the Pt wires modified with $[N(C_{18}H_{37})(CH_3)_3]Cl$. The wires are well dispersed compared to the surfactant-free wires. Modification with $P(C_6H_5)_3$ gives nanowire arrays (Figure 8d). In the EDS analysis of the arrays, P and Pt were detected in ca. 65 and 30 atom %, respectively, but neither Si nor F was observed. In Figure 8d, the distance between the adjacent wires is ca. 3 nm, which is slightly longer than the distance (1.0−1.5 nm) between the $P(C_6H_5)_3$-free wires (Figure 8a,b). By consideration of these results, it is suggested that the Pt wires are covered with several layers of $P(C_6H_5)_3$. In contrast to the ligand-free Pt wires, the $P(C_6H_5)_3$-modified wires are stable in ethanol at 278 K. Figure 8e is an HRTEM image of a $P(C_6H_5)_3$-modified Pt wire, and two types of lattice fringes are clearly seen. The fringes are ascribed to {111} and {200} planes, because the d spacings are 0.233 and 0.202 nm and the dihedral angle is 54°. These data indicate that the wires have high crystallinity.[10]

STM images of the ligand-free Pt wires are shown in Figure 9. By comparing the morphology, we note that the Pt wire from pure siliceous FSM-16 has smooth surface with a rodlike structure (diameter 3 nm) but the Pt wires from HMM-1 have an uneven surface with a necklace-like structure. Each particle unit is 3 nm in diameter and 4 nm in length. Although the HRTEM studies suggested the necklace structure (Figure 8c,e and ref 32), the STM data clearly show the difference of surface structures. We believe that the metal−support interaction of Pt with the internal surface of HMM is weaker than that with pure

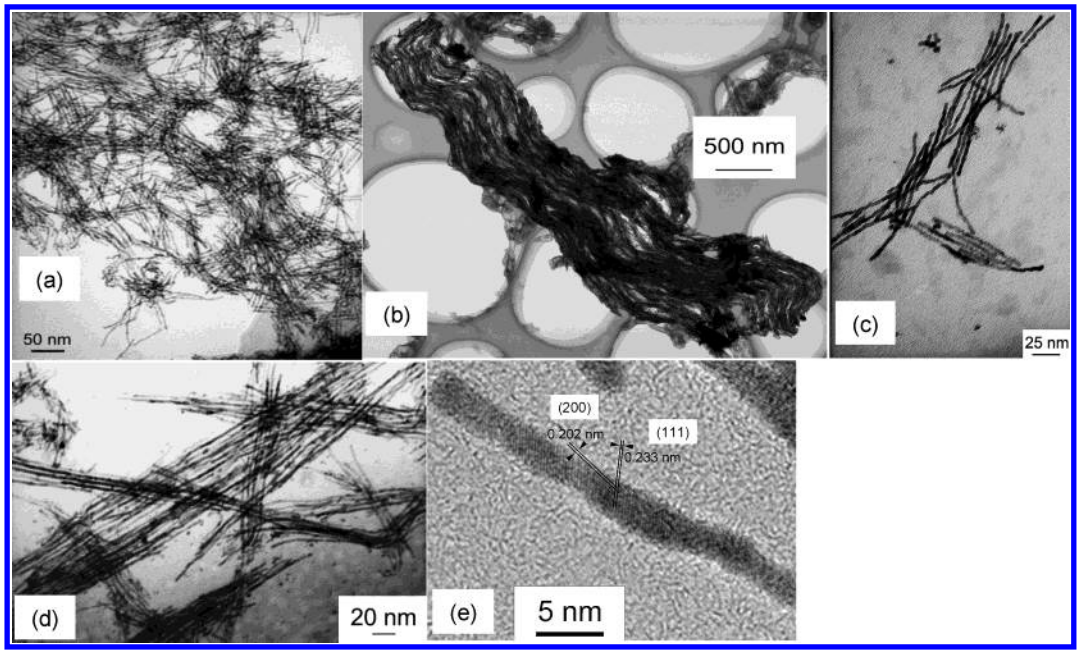

Figure 8. TEM images of unsupported Pt wires: (a) ligand-free Pt wires; (b) low-magnification image of ligand-free Pt wires; (c) $[N(C_{18}H_{37})(CH_3)_3]Cl$-modified Pt wires; (d) $P(C_6H_5)_3$-modified Pt wires; (e) HRTEM image of a $P(C_6H_5)_3$-modified Pt wire.

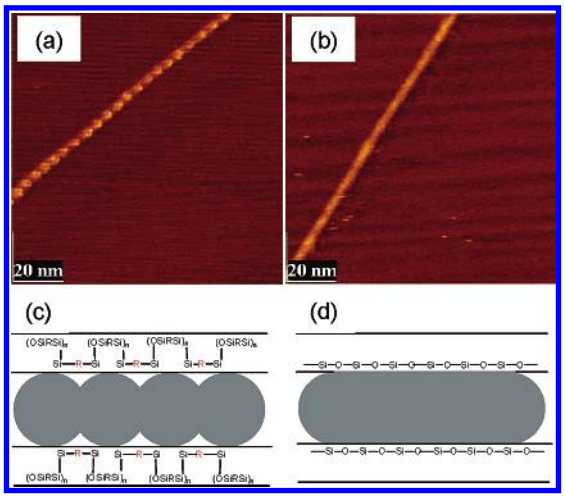

Figure 9. STM images of isolated Pt wires on HOPG and structural models of occluded wires: (a) Pt nanonecklace separated from HMM-1; (b) Pt nanorod separated from FSM-16; (c) Pt nanonecklace in HMM-1; (d) Pt nanorod in FSM-16.

silica surface of FSM-16 (Figure 9c,d). This results in the increase in the surface energy of Pt metal to give the nanonecklace structure.

Conclusion

We have demonstrated that Pt nanowires can be synthesized in HMM-1 templates in high yields by the photoreduction method. From the mechanistic study, it is revealed that the migration of Pt species in water/methanol phase is the key to successful growth of Pt wires. The photoreduction is a simple and reproducible method to prepare the Pt wires with high aspect ratio, while thermal H_2-reduction needs careful control of the reaction conditions. The isolation of Pt wires is possible by removing HMM-1 with HF, and it is confirmed that the wire has a nanonecklace structure. We have shown that the unsupported Pt wires are stabilized by modification with ligands. The ligand-modified nanowires would have a broad range of applications in the fabrication of highly ordered nanostructures.

Acknowledgment. This work was partially supported by a Grant-in-Aid for Scientific Research from the Ministry of Education, Science, Sports and Culture, Japan (Grant Nos. 13650836 and 14340213). We thank Prof. O. Terasaki and Dr. S. Suzuki for helpful discussion on the structural characterization of Pt nanowires.

Supporting Information Available: Figures of a reaction setup for photoredcution and XRD patterns of Pt/HMM-1 after UV-irradiation for 0−48 h (PDF format). This material is available free of charge via the Internet at http://pubs.acs.org.

References and Notes

(1) Hu, J.; Odom, T. W.; Lieber, C. M. *Acc. Chem. Res.* **1999**, *32*, 435−445.
(2) Zach, M. P.; Ng, K. H.; Penner, R. M. *Science* **2000**, *290*, 2120−2123.
(3) El-Sayed, M. A. *Acc. Chem. Res.* **2001**, *34*, 257−264.
(4) Foss, C. A.; Hornyak, G. L.; Stockert, J. A.; Martin, C. R. *J. Phys. Chem.* **1992**, *96*, 7497−7499.
(5) Yanagisawa, T.; Shimizu, T.; Kuroda, K.; Kato, C. *Bull. Chem. Soc. Jpn.* **1990**, *63*, 988−992.
(6) Inagaki, S.; Fukushima, Y.; Kuroda, K. *J. Chem. Soc., Chem. Commun.* **1993**, 680−682.
(7) Kresge, C. T.; Leonowicz, M. E.; Roth, W. J.; Vartuli, J. C.; Beck. J. S. *Nature* **1992**, *359*, 710−712.
(8) Zhao, D.; Feng, J.; Huo, Q.; Melosh, N.; Fredrickson, G. H.; Chmelka, B. F.; Stucky, G. D. *Science* **1998**, *279*, 548−552.
(9) Ko, C. H.; Ryoo, R. *Chem. Commun.* **1996**, 2467−2468.
(10) Liu, Z.; Sakamoto, Y.; Ohsuna, T.; Hiraga, K.; Terasaki, O.; Ko. C. H.; Shin, H. J.; Ryoo, R. *Angew. Chem., Int. Ed.* **2000**, *39*, 3107−3110.
(11) Han, Y.-J.; Kim, J. M.; Stucky, G. D. *Chem. Mater.* **2000**, *12*, 2068−2069.
(12) Huang, M. H.; Choudrey, A.; Yang, P. *Chem. Commun.* **2000**, 1063−1064.
(13) Coleman, N. R. B.; Morris, M. A.; Spalding, T. R.; Holmes, J. D. *J. Am. Chem. Soc.* **2001**, *123*, 187−188.
(14) Lee, K.-B.; Lee, S.-M., Cheon, J. *Adv. Mater.* **2001**, *13*, 517−520.
(15) Yang, C.-M.; Sheu, H.-S.; Chao, K.-J. *Adv. Funct. Mater.* **2002**, *12*, 143−148.
(16) Ichikawa, M. In *Metal Clusters and Catalysis*; Braunstein, P., Oro, L. A., Raithby, P. R., Eds.; Wiley-VCH: Weinheim, Germany, 1999; pp 1273−1301.
(17) Ichikawa, M. *Adv. Catal.* **1992**, *38*, 283−400.
(18) Sasaki, M.; Osada, M.; Sugimoto, N.; Inagaki, S.; Fukushima, Y.; Fukuoka, A.; Ichikawa, M. *Microporous Mesoporous Mater.* **1998**, *21*, 597−606.

(19) Sasaki, M.; Osada, M.; Higashimoto, N.; Yamamoto, T.; Fukuoka, A.; Ichikawa, M. *J. Mol. Catal. A* **1999**, *141*, 223−240.

(20) Fukuoka, A.; Higashimoto, N.; Sakamoto, Y.; Sasaki, M.; Sugimoto, N.; Inagaki, S.; Fukushima, Y.; Ichikawa, M. *Catal. Today* **2001**, *66*, 23−31.

(21) Fukuoka, A.; Higashimoto, N.; Sakamoto, Y.; Inagaki, S.; Fukushima, Y.; Ichikawa, M. *Microporous Mesoporous Mater.* **2001**, *48*, 171−179.

(22) Fukuoka, A.; Higashimoto, N.; Sakamoto, Y.; Inagaki, S.; Fukushima, Y.; Ichikawa, M. *Top. Catal.* **2002**, *18*, 73−78.

(23) Fukuoka, A.; Araki, H.; Sakamoto, Y.; Sugimoto, N.; Tsukada, H.; Kumai, Y.; Akimoto, Y.; Ichikawa, M. *Nano Lett.* **2002**, *2*, 69−75.

(24) Araki, H.; Fukuoka, A.; Sakamoto, Y.; Inagaki, S.; Sugimoto, N.; Fukushima, Y.; Ichikawa, M. *J. Mol. Catal. A* **2003**, *199*, 95−102.

(25) Inagaki, S.; Guan, S.; Fukushima, Y.; Ohsuna, T.; Terasaki, O. *J. Am. Chem. Soc.* **1999**, *121*, 9611−9614.

(26) Guan, S.; Inagaki, S.; Ohsuna, T.; Terasaki, O. *J. Am. Chem. Soc.* **2000**, *122*, 5660−5661.

(27) Inagaki, S.; Guan, S.; Ohsuna, T.; Terasaki, O. *Nature* **2002**, *416*, 304−307.

(28) Kapoor, M. P.; Yang, Q.; Inagaki, S. *J. Am. Chem. Soc.* **2002**, *124*, 15176−14177.

(29) Melda, B. J.; Holland, B. T.; Blanford, C. F., Stein, A. *Chem. Mater.* **1999**, *11*, 3302−3308.

(30) Yoshina-Ishii, C.; Asefa, T.; Coombs, N.; MacLachlan, M. J.; Ozin, G. A. *Chem. Commun.* **1999**, 2539−2540.

(31) Asefa, T.; MacLachlann; Coombs, N.; Ozin, G. A. *Nature* **1999**, *402*, 867−871.

(32) Fukuoka, A.; Sakamoto, Y.; Guan, S.; Inagaki, S.; Sugimoto, N.; Fukushima, Y.; Hirahara, K.; Iijima, S.; Ichikawa, M. *J. Am. Chem. Soc.* **2001**, *123*, 3373−3374.

(33) Fukuoka, A.; Araki, H.; Sakamoto, Y.; Inagaki, S.; Fukushima, Y.; Ichikawa, M. *Inorg. Chim. Acta* **2003**, *350*, 371−378.

(34) Zhang, Z.; Ying, J. Y.; Dresselhaus, M. S. *J. Mater. Res.* **1998**, *13*, 1745−1748.

(35) Yu, J.; Kim, J. Y.; Lee, S.; Mbondyo, J. K. N.; Martin, B. R.; Mallouk, T. E. *Chem. Commun.* **2000**, 2445−2446.

(36) Lago, R. M.; Tsang, S. C.; Lu, K. L.; Chen, Y. K.; Green, M. L. H. *Chem. Commun.* **1995**, 1355−1356.

(37) Sloan, J.; Hammer, J.; Zwiefka-Sibley, M.; Green, M. L. H. *Chem. Commun.* **1998**, 347−348.

(38) Govindaraj, A.; Satishkumar, B. C.; Nath, M.; Rao, C. N. R. *Chem. Mater.* **2000**, *12*, 202−205.

(39) Grobert, N.; Mayne, M.; Terrones, M.; Sloan, J.; Dunin-Borkowski, R. E.; Kamalakaran, R.; Seeger, T.; Terrones, H.; Rühle, M.; Walton, D. R. M.; Kroto, H. W.; Hutchinson, J. L. *Chem. Commun.* **2001**, 471−472.

(40) Kyotani, T.; Tsai, L.; Tomita, A. *Chem. Commun.* **1997**, 701−702.

(41) Bradley, J. S. In *Clusters and Colloids*; Schmid, G., Ed.; VCH: Weinheim, Germany, 1994; pp 459−544.

(42) Michaelis, M.; Henglein, A. *J. Phys. Chem.* **1992**, *96*, 4719−4724.

(43) Shin, H. J.; Ryoo, R.; Liu, Z.; Terasaki, O. *J. Am. Chem. Soc.* **2001**, *123*, 1246−1247.